

Non-contact, ultrasound-based indentation method for measuring elastic properties of biological tissues using Harmonic Motion Imaging (HMI)

This content has been downloaded from IOPscience. Please scroll down to see the full text.

2015 Phys. Med. Biol. 60 2853

(<http://iopscience.iop.org/0031-9155/60/7/2853>)

View [the table of contents for this issue](#), or go to the [journal homepage](#) for more

Download details:

IP Address: 156.145.114.120

This content was downloaded on 06/11/2015 at 18:26

Please note that [terms and conditions apply](#).

Non-contact, ultrasound-based indentation method for measuring elastic properties of biological tissues using Harmonic Motion Imaging (HMI)

Jonathan Vappou^{1,2}, Gary Y Hou², Fabrice Marquet²,
Danial Shahmirzadi², Julien Grondin², and
Elisa E Konofagou^{2,3}

¹ ICube, Université de Strasbourg, CNRS, France

² Ultrasound and Elasticity Imaging Laboratory, Department of Biomedical Engineering, Columbia University, New York, NY 10027, USA

³ Department of Radiology, Columbia University, New York, NY 10027, USA

E-mail: ek2191@columbia.edu

Received 23 October 2014, revised 15 January 2015

Accepted for publication 4 February 2015

Published 17 March 2015



Abstract

Noninvasive measurement of mechanical properties of biological tissues *in vivo* could play a significant role in improving the current understanding of tissue biomechanics. In this study, we propose a method for measuring elastic properties non-invasively by using internal indentation as generated by harmonic motion imaging (HMI). In HMI, an oscillating acoustic radiation force is produced by a focused ultrasound transducer at the focal region, and the resulting displacements are estimated by tracking radiofrequency signals acquired by an imaging transducer. In this study, the focal spot region was modeled as a rigid cylindrical piston that exerts an oscillatory, uniform internal force to the underlying tissue. The HMI elastic modulus E_{HMI} was defined as the ratio of the applied force to the axial strain measured by 1D ultrasound imaging. The accuracy and the precision of the E_{HMI} estimate were assessed both numerically and experimentally in polyacrylamide tissue-mimicking phantoms. Initial feasibility of this method in soft tissues was also shown in canine liver specimens *in vitro*. Very good correlation and agreement was found between the measured Young's modulus and the HMI modulus in the numerical study ($r^2 > 0.99$, relative error $< 10\%$) and on polyacrylamide gels ($r^2 = 0.95$, relative error $< 24\%$). The average HMI modulus on five liver samples was found to $E_{\text{HMI}} = 2.62 \pm 0.41$ kPa, compared to $E_{\text{MechTesting}} = 4.2 \pm 2.58$ kPa measured by rheometry. This study has demonstrated for the

first time the initial feasibility of a non-invasive, model-independent method to estimate local elastic properties of biological tissues at a submillimeter scale using an internal indentation-like approach. Ongoing studies include *in vitro* experiments in a larger number of samples and feasibility testing in *in vivo* models as well as pathological human specimens.

Keywords: ultrasound, elasticity imaging, harmonic motion imaging, Young's modulus, strain estimation, finite element analysis, mechanical testing

(Some figures may appear in colour only in the online journal)

1. Introduction

Measuring material properties with noninvasive, nondestructive methods has always been a challenging field in materials science. This is particularly true for biological tissues, where conventional mechanical testing methods are external and limited to either superficial tissues or to *in vitro* testing (Fung 1967, Holzapfel *et al* 2000, Sakuma *et al* 2003, Haslach 2005) and hence, do not allow to measure mechanical properties of major organs *in vivo*.

Elasticity Imaging is a research field that has been continuously expanding since its initial development more than two decades ago. The initial objective of such methods was to combine the principle of palpation with medical imaging modalities. Research in this field has developed beyond the sole initial objective of diagnosis by mechanical excitation, and a large number of methods have been proposed that offer more complex applications. In particular, there has been an increasing interest in the use of elasticity imaging methods for quantifying several aspects of biomechanics, as imaging offers the valuable advantage of measuring mechanical properties *in vivo* in a noninvasive manner. Examples of the use of elasticity imaging methods for biomechanical applications include: magnetic resonance elastography (MRE) for the determination of brain and liver tissue viscoelastic properties *in vivo* (Klatt *et al* 2007, Atay *et al* 2008, Green *et al* 2008), evaluation of differences in elastic properties between brain tissue white and grey matter (Pattison *et al* 2010) and comparison between *in vivo* and post-mortem brain properties (Vappou *et al* 2008); MRE for the measurement of skeletal muscle contraction and muscle stiffness changes with aging (Jenkyn *et al* 2003, Domire *et al* 2009); Transient Elastography to assess skeletal muscle stiffness during contraction (Gennisson *et al* 2005); Dynamic ultrasound elastography for the rheological characterization of blood clots (Viola *et al* 2004, Schmitt *et al* 2011); Shear Waving Elasticity Imaging (SWEI) and Supersonic Shear Imaging (SSI) for the measurement of shear wave dispersion and characterization of soft tissue viscoelasticity (Sarvazyan *et al* 1998, Deffieux *et al* 2009); acoustic radiation force impulse (ARFI) Imaging for evaluating stiffness of *in vivo* liver (Palmeri *et al* 2008) and *ex vivo* colon cancer specimens based on tissue relaxation characteristics following acoustic radiation force excitation (Zhai *et al* 2008); shear-wave dispersion ultrasound vibrometry (SDUV) for investigation of *in vivo* viscoelastic properties in porcine liver (Chen *et al* 2004, 2009). The reader is referred to review papers in the field of elasticity imaging for more details about this fast-growing field (Mariappan *et al* 2010, Vappou 2012). This paper introduces another new ultrasound-based method for the measurement of the tissues elasticity, based on the principle of indentation.

Indentation is a widely used material testing method that allows to measure the Load-Displacement curve. Analytical solutions were proposed by Sneddon (Sneddon 1965) in the

case of penetration of axisymmetric indentors in an elastic half space. Based on these relationships, several methods have been proposed to derive the Young's modulus of the tested material. For example, as proposed by Oliver and Pharr (Oliver and Pharr 1992), the Young's modulus can be estimated using a complex iterative procedure and calibration process. While indentation is commonly used for materials such as polymers and metallic samples, the applications of such experimental approaches are limited *in vivo*, due to the external nature of indentation. Instead, we hereby propose a non-invasive internal indentation method that uses the acoustic radiation force resulting from focused ultrasound and the simultaneous measurement of the resulting displacement, using therefore the basic principle of the Harmonic Motion Imaging (HMI) method (Maleke *et al* 2006). A stiffness index named as the HMI modulus (E_{HMI}) is estimated using the applied acoustic radiation force divided by the resulting deformations measured using radiofrequency (RF) signal processing. The HMI modulus is compared to the actual Young's modulus on both tissue-mimicking phantoms and *in vitro* biological specimens.

Harmonic motion imaging (HMI) is an ultrasound-based method that uses an amplitude modulated (AM) signal in order to generate an oscillating radiation force at the focal region using a focused ultrasound (FUS) transducer. The original objective of HMI was to constitute an all-in-one tool for tumor detection, characterization, targeting and monitoring of the thermal ablation. Within the small focal region (typically few mm^3), force density oscillates at a single frequency within typically the 10–200 Hz range. At the same time, an imaging transducer that is concentric and confocal with the FUS transducer is simultaneously operated to acquire ultrasound RF data during the FUS excitation. Displacements resulting from the oscillating acoustic radiation force are estimated by using cross-correlation techniques on consecutively acquired ultrasound RF signals during force application. This paper investigates a new role for HMI, namely, a mechanical testing tool, where a known dynamic force density is applied and the resulting displacement is measured. The objectives of this paper are thus to (1) introduce a stiffness index, namely, the HMI modulus E_{HMI} , based on the applied force and on the measured strains, (2) assess the level of agreement between E_{HMI} and the true Young's modulus E with finite-element simulations, (3) assess the quality and the experimental feasibility of the proposed method on phantoms, by comparing E_{HMI} to the Young's modulus measured by mechanical testing, and (4) demonstrate feasibility of the proposed method on *ex vivo* biological tissues. The general objective of the proposed method is to provide an HMI-based mechanical testing setup that is particularly relevant for biomechanics as it is non-contact, non-invasive, and it can be used *in vivo*.

2. Materials and methods

2.1. Calculation of the HMI elastic modulus

The method is based on the localized, internal acoustic radiation force, instead of an external mechanical indenter, as the source of stress. In HMI, a focused ultrasound (FUS) transducer is used to generate an oscillatory force at the focal region. The force density can be measured experimentally as part of the transducer calibration, and its spatial profile can therefore be known. The resulting displacement is measured using the consecutive RF signals acquired during the application of the oscillatory force. The general experimental setup is summarized in figure 1(a).

In the proposed method, the focal region is modeled as a cylindrical region inside which the volumetric acoustic radiation force is uniform. This is an approximation that will be further addressed in this manuscript since the actual radiation force has a well-defined spatial

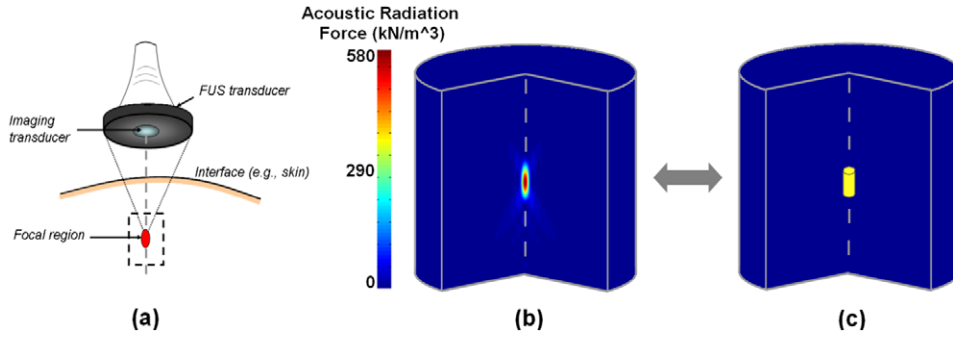


Figure 1. (a) General HMI setup, (b) actual distribution of the volumic acoustic radiation force field, and (c) equivalent volumic force modeled as uniform within the focal region.

distribution (figures 1(b) and (c)). This cylindrical region is therefore assumed to act as an oscillating rigid piston.

Under the assumption of linear elasticity, the balance of forces on the z -axis acting on this cylindrical region can be written as:

$$\rho \frac{\partial^2 u_z}{\partial t^2} V = \iiint_V f_V dV - F_{\text{shear}} - F_{\text{top}} - F_{\text{bottom}} \tag{1}$$

F_{shear} , F_{top} and F_{bottom} correspond to the vertical forces acting on the lateral, superior and inferior surfaces of the cylinder, respectively (cf figure 2). V is the volume of the cylinder, u_z is the vertical displacement of the cylinder, ρ is the density of the tissue and f_V is the local, volumic acoustic radiation force. The inertia term on the left side of the equation is considered negligible (1), as its order of magnitude is approximately 0.1% of the one of the other terms within the typical HMI frequency range (10–50 Hz). Therefore, equation (1) can be rewritten as:

$$\iiint_V f_V dV = F_{\text{shear}} + F_{\text{top}} + F_{\text{bottom}}, \tag{2}$$

which can be simply deemed as a static balance of forces, where the applied acoustic radiation force equals the sum of elastic forces related to the deformation of the tissue around the piston:

$$\begin{cases} F_{\text{top}} = F_{\text{bottom}} = \pi R^2 * E \frac{\partial u_z}{\partial z} \\ F_{\text{shear}} = 2\pi R h * G \frac{\partial u_z}{\partial r} \end{cases} \tag{3}$$

where R , h denote the radius and the height of piston, respectively, and E , G denote the Young's and shear modulus of the tissue, respectively. Under the assumption of quasi-incompressibility ($E = 3G$), equation (2) becomes:

$$\iiint_V f_V dV = E * \left(2\pi R^2 * \frac{\partial u_z}{\partial z} + \frac{1}{3} 2\pi R h * \frac{\partial u_z}{\partial r} \right). \tag{4}$$

Equation (4) can be rewritten with tensorial strain components:

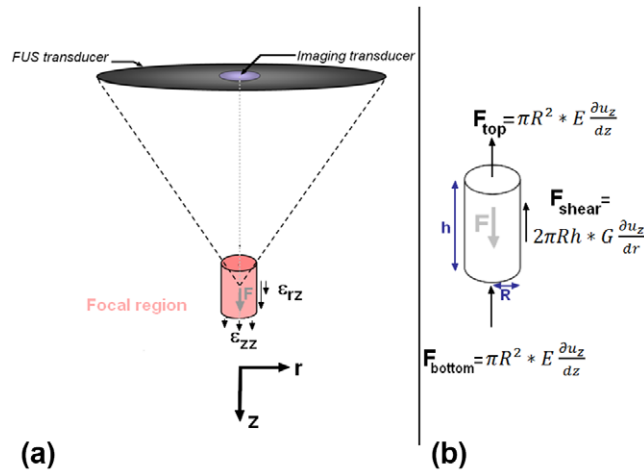


Figure 2. (a) Illustration of the focal region as a cylindrical piston exerting a vertical force, and corresponding deformations of the surrounding tissue, (b) illustration of the forces acting on this cylinder.

$$\iiint_v f_v dV = 2E\pi R * \left(R * \epsilon_{zz} + \frac{2}{3}h * \epsilon_{rz} \right), \tag{5}$$

which assumes that the displacement occurs along the z -axis only with $\epsilon_{rz} = 1/2 (\partial u_z / \partial r)$.

Another major assumption in this study is that the compressive and shear strains are equal. As it will be demonstrated in the numerical study, they are indeed very close in a cylindrical geometry as the one used here. Consequently, equation (5) can be written as:

$$\iiint_v f_v dV = 2E\pi R \epsilon_{zz} * \left(R + \frac{2}{3}h \right). \tag{6}$$

Finally, we define our HMI modulus as:

$$E_{HMI} = \frac{\iiint_v f_v dV}{2\pi R \epsilon_{zz} * \left(R + \frac{2}{3}h \right)}. \tag{7}$$

The HMI elastic modulus method requires knowledge of the acoustic radiation force. In this study, we used the experimental pressure profile obtained using a needle hydrophone in water, as described elsewhere (Maleke *et al* 2010). The acoustic radiation force f_{exp} was then calculated as:

$$f_{exp} = \frac{2\alpha I}{c_s}, \tag{8}$$

where I is the acoustic intensity, c_s the speed of sound ($c_s = 1530 \text{ m s}^{-1}$), and α the acoustic absorption of the medium, which was assumed to be equal to the acoustic attenuation. The attenuation of the tissue ahead of the focus was taken into account in order to obtain realistic estimates of the acoustic intensity at the focus. The corresponding 3D acoustic radiation force distribution was used as the input in both simulations and experiments throughout the study.

2.2. Numerical study

Finite-element simulations were performed using a commercial software package (Comsol Multiphysics 4.3). This numerical study had principally three objectives, namely (1) to validate the underlying theory summarized by equation (7), and to evaluate differences between E_{HMI} and the actual Young's modulus numerically; (2) To evaluate the estimation error resulting from the assumption of a uniform cylindrical piston, by comparing results obtained using the actual experimental force field; (3) To assess the estimation error resulting from assumption of a uniform medium, by adding heterogeneities of different sizes.

In all studies shown, axisymmetric models were used, and the geometry of the medium was chosen as cylindrical (50 mm in height by 50 mm in diameter). All problems were solved as static, the input force being equal as the maximum of the oscillatory force. The focal region was set at the center of the axis of revolution with mesh refinement around this focal region.

2.2.1. Evaluation of the differences between E_{HMI} and Young's modulus. This section aimed at investigating the reliability of the underlying theory that allows the estimation of the elastic modulus as summarized by equation (7). The numerical phantom was considered as uniform. Its Young's modulus E was varied across a range representing typical stiffness of the soft tissue (0.5, 1, 2.5, 5, 10, 25, 50, 100 kPa). The dimensions of the cylindrical piston were chosen as the zone inside which the volumetric force is greater than 10% of the maximum force using experimental beam profiles, resulting in a region of 3 mm in height and 1.5 mm in diameter. The input force was implemented as uniform within this cylinder, and equal to the spatial average of the experimentally-measured force. For each case, the axial strain was averaged over a small rectangular region of interest (ROI) immediately below the focus (1.5 mm in diameter, 1 mm in height), in order to estimate the HMI modulus using equation (7).

2.2.2. Evaluation of the approximation of uniform radiation force density distribution. The proposed method to estimate the Young's modulus, summarized by equation (7), assumes that the cylindrical piston is perfectly rigid, i.e. that the distribution of the volumic force inside this piston is perfectly uniform. In reality, the spatial distribution of the acoustic radiation force is non-uniform, despite the fact that virtually all of the energy is concentrated in the focal spot region. Here, we evaluate the error related to the assumption of uniformity of the force. The same simulations were performed as in the previous subsection under two different conditions: (1) using the true, experimentally-measured spatial force distribution and (2) using the equivalent rigid piston with a uniform force equal to the spatial average of the actual force, as required by the theory. It is important to emphasize that the total force, defined as the integration of the volumic force within the piston volume, is identical in the two cases. The Young's modulus of the medium was chosen equal to $E = 10$ kPa.

2.2.3. Influence of heterogeneity. Our method assumes that the tested tissue is uniform. Here, we evaluated the error resulting from the fact that the tissue around the focal region could not be perfectly uniform. A spherical inclusion with different mechanical properties was added around the focal region. The background stiffness was fixed to $E_{\text{background}} = 5$ kPa while $E_{\text{inclusion}} = 20$ kPa. The diameter of the inclusion was varied between 2 and 10 mm. E_{HMI} was calculated for each case.

2.3. Tissue mimicking phantom study

The 1D HMI modulus was measured on six polyacrylamide (PA) phantoms (concentrations of 15, 20, 25, 30, 35 and 40%), and compared to the Young's modulus measured by mechanical

testing. For each gel, the same liquid mixture (before cross-linking) used for the construction of HMI phantoms was used to make samples for mechanical testing. For the HMI experiments, parallelepiped-shaped phantoms were prepared (approx. 10 cm by 5 cm by 5 cm). Agar powder (4%) was added to each mixture for scattering. The HMI experimental protocol used here has been described in details previously (Maleke *et al* 2006). The amplitude-modulated (AM) frequency was 20 Hz, resulting in an excitation frequency of $f = 40$ Hz. The HMI system was comprised of a PZT HIFU 4.5 MHz transducer (outer diameter 80 mm, inner diameter 16.5 mm, focal depth 9 cm, Riverside Research Institute, New York, NY) and a confocal 7.5 MHz single-element pulse-echo transducer (Olympus-NDT, Waltham, MA, US) with a diameter of 15 mm and a focal length of 6 cm for simultaneous RF signals acquisition at a frame rate of 4 kHz. The focal region was approximately at 1.25 cm depth from the surface of the gel. Displacements were measured using cross-correlation on raw ultrasonic RF signals. The size of the window for displacement estimation was equal to 1.8 mm, with an overlap of 90%. The compressive strain was calculated using a 1st derivative Savitzky–Golay filter (kernel = 7). Figure 3 illustrates how strain is calculated from displacement images. Absorption α was measured by transmission. It was found to be equal to $\alpha = 0.25 \text{ cm}^{-1}$ at $f_{\text{center}} = 4.5 \text{ MHz}$.

2.4. HMI modulus study on *ex vivo* specimens

Canine liver specimens (lobe = 2, location = 5) were excised immediately upon sacrifice. All procedures were approved by the Institutional Animal Care and Use Committee of Columbia University. The tissue specimens were immersed in a degassed Phosphate Buffered Saline (PBS) bath upon excision and throughout the experimental procedure. Both the HMI and experimental protocols used here have been described in details previously (Maleke and Konofagou 2008) where the AM frequency was 25 Hz, resulting in an excitation frequency of $f = 50$ Hz. The HIFU transducer had a center frequency of 4.75 MHz, an outer diameter and inner diameter of 80 and 16.5 mm, respectively, and its focal depth was 9 cm (Riverside Research Institute, New York, NY). The transducer was positioned in such a way that the end of axial focal zone (i.e. the region where the axial compressive strain can be estimated) was well within the liver specimen. The focal region was approximately at 1.5 cm depth from the surface of the liver. The compressive strain was calculated using a 1st derivative Savitzky–Golay filter (kernel = 7). The size of the window for displacement estimation was equal to 1.05 mm, with an overlap of 95%. The absorption value for force calculation from *ex vivo* studies was chosen to be $\alpha = 0.75 \text{ cm}^{-1}$ at $f_{\text{center}} = 4.5 \text{ MHz}$ based on previous literature (Hou *et al* 2011).

2.5. Mechanical testing

2.5.1. Polyacrylamide phantoms. Cylindrically-shaped samples were prepared for each gel ($N = 5$ –8 per gel, diameter = 12 mm, thickness = 2.5 to 3.5 mm) used in the study. The samples were tested on an ARES rheometer (TA Instruments, NewCastle, DE, USA). Dynamic analysis was performed at frequencies between 1 and 10 Hz at $\epsilon = 0.5\%$ strain. The value of the shear storage modulus $G_{\text{Mech. Test.}}$ measured at $f_{\text{AM}} = 10 \text{ Hz}$ was selected as the reference value, and the Young's modulus was obtained by $E_{\text{Mech. Test.}} = 3 G_{\text{Mech. Test.}}$ under the assumption of quasi-incompressibility.

2.5.2. Liver samples. Samples were collected from the same livers as those tested by HMI, and were constantly kept in Phosphate Buffered Saline (PBS) (Fisher Scientific, Pittsburgh, PA) during *ex vivo* transportation and mechanical testing. To minimize the variations in tissue

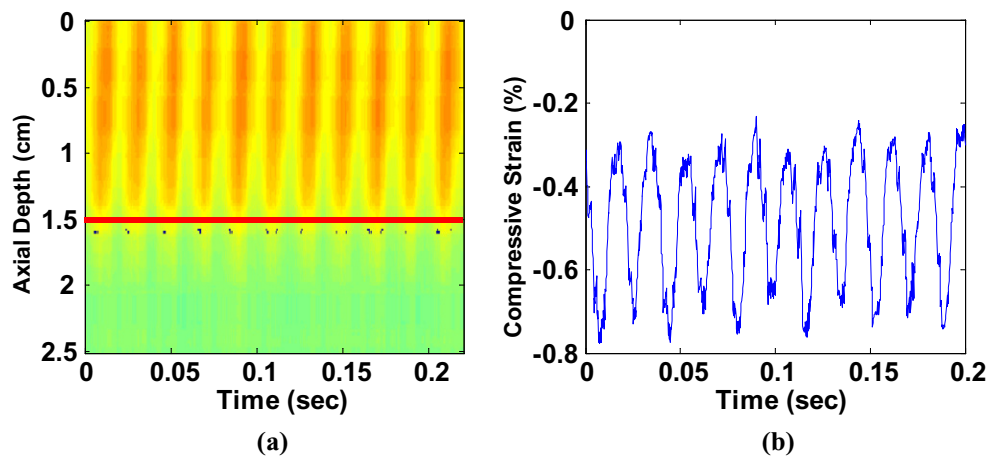


Figure 3. (a) Estimated displacement using 1D cross correlation, and (b) estimated axial compressive strain. The red line indicates the region of investigation for compressive strain, i.e. end of acoustic focal zone. Note that the displacement profile is plotted in m-mode.

properties, all tests were completed within 12h post-mortem. Five cylindrical test specimens of diameter $d = 5.19 \pm 0.41$ mm and height $h = 4.22 \pm 0.80$ mm ($N = 3$ and $N = 2$ for liver 1 and 2, respectively) were prepared using a biopsy punch. The specimens remained unconfined between the top/bottom plates, pre-compressed (to induce enough grip between the tissue and grip surfaces) ($\epsilon = 5\%$), and tested under oscillatory shear test ($\epsilon = 1\%$, $f = 1\text{--}10$ Hz) in order to measure the shear modulus ($G_{\text{Mech. Test.}}$). The value of the shear storage modulus $G_{\text{Mech. Test.}}$ measured at $f = 10$ Hz was chosen as the reference value, and the Young's modulus was obtained by $E_{\text{Mech. Test.}} = 3 G_{\text{Mech. Test.}}$ under the assumption of quasi-incompressibility.

3. Results

3.1. Numerical study

3.1.1. Evaluation of the differences between E_{HMI} and Young's modulus. The HMI modulus E_{HMI} was calculated from equation (7) using the output of finite-element simulations. Excellent correlation was found between the actual Young's modulus E and E_{HMI} ($r^2 > 0.99$). E and E_{HMI} were found to be very close, as described in table 1. The relationship between them was found to be: $E_{\text{HMI}} = 0.915 * E - 60$ (Pa), illustrating that E_{HMI} estimates are slightly but systematically lower than E .

3.1.2. Evaluation of the approximation of uniform radiation force density distribution. E_{HMI} values were compared in two cases, namely, (1) using the actual force density field derived from experimental measurements and (2) using the corresponding modeled force field uniform within the focal region. Figure 4 illustrates the strain profile around the focal region (zoomed) for both cases. The values of ϵ_{zz} in the uniform case differ from the ϵ_{zz} measured using the actual force density field, but this difference was deemed to be relatively limited ($\approx 12\%$ relative error).

3.1.3. Dependence on heterogeneity. The inclusion size was varied between 4 and 20 mm in diameter (focal region height = 3 mm). For an inclusion size of 6 mm or higher, the HMI

Table 1. Results from simulations on uniform phantoms whose Young's modulus is varied between 0.5 and 100 kPa, and corresponding HMI modulus found by using equation (7).

Input Young's modulus (kPa)	Axial strain ϵ_{zz}	Shear strain ϵ_{rz}	E_{HMI} calculated from equation (7), kPa	Relative error (%)
0.5	0.203	0.196	0.45	10
1	0.1	0.975	0.914	8.6
2.5	0.04	0.038	2.25	10
5	0.02	0.019	4.57	8.6
10	0.01	0.098	9.05	9.5
25	0.004	0.0039	22.7	9.2
50	0.002	0.0019	45.2	9.6
100	0.001	0.0096	91.3	8.7

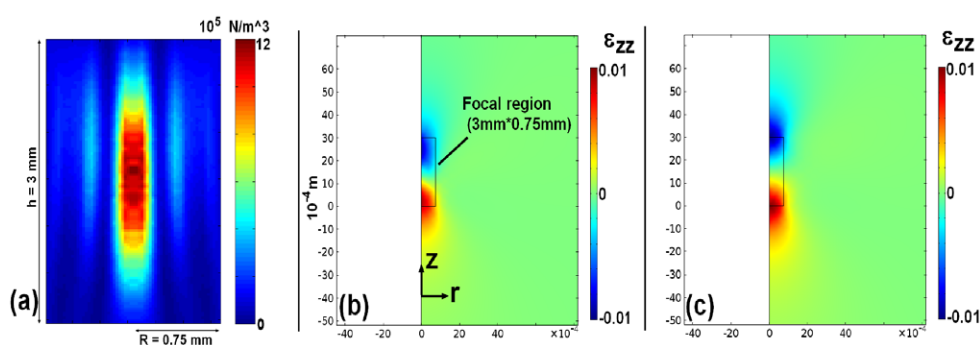


Figure 4. (a) Volumic force profile implemented in simulations from experimental pressure measurements, (b) resulting axial strain using this profile and (c) axial strain obtained using the equivalent uniform force profile (where the force value is the spatial average of (a)).

modulus was found to be very similar to the HMI modulus found in the uniform case (<10% relative error). For inclusion sizes smaller than 6 mm, the HMI modulus was found to be significantly different (figure 5). This difference was equal to 22% in the 4 mm inclusion size. These results are indicative of the fact that as long as a heterogeneity is larger than ~6 mm, it will have very limited influence on the estimated E_{HMI} and we will estimate the E_{HMI} of this inclusion. If the heterogeneity is smaller than ~6 mm, the calculated E_{HMI} is affected by both the elasticity of the inclusion and of the background.

3.2. Tissue-mimicking phantom study

Excellent correlation ($r^2 = 0.95$) was found between the Young's modulus and HMI modulus. Figure 6 illustrates the HMI modulus versus the Young's modulus for the 6 tested gels. The linear relationship between E and E_{HMI} was found as $E_{\text{HMI}} = 0.83 * E + 0.51$ (kPa).

3.3. Ex vivo liver study

The estimated E_{HMI} and the Young's Modulus measured on all liver specimens are listed on tables 2 and 3. The average value of the HMI modulus was found to 2.62 ± 0.41 kPa whereas the measured Young's Modulus from mechanical testing was 4.20 ± 2.58 kPa.

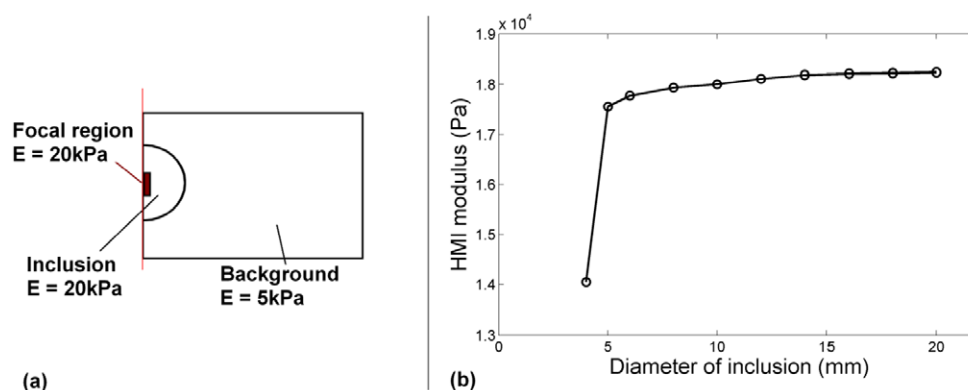


Figure 5. Effect of the size of the inclusion on the estimated HMI modulus. (a) Description of the geometry used for the simulation; (b) HMI modulus versus size of the inclusion. E_{HMI} in the uniform case is equal to 18.4 kPa (corresponding to input $E = 20$ kPa).

4. Discussion

In this paper, a methodology for internal, non-contact indentation of soft tissues using HMI was proposed and investigated both theoretically and experimentally. Currently, there are no techniques available for a localized, noninvasive, internal, indentation-based assessment of mechanical properties for biological specimens. Based on the principle of HMI, our proposed method utilized the applied force and measured the resulting deformation. We hereby propose a stiffness modulus, namely, the HMI modulus (E_{HMI}). We initiated our study from numerical simulation, followed by a feasibility study using tissue-mimicking phantoms, and *ex vivo* canine liver samples. We compared our findings against those obtained by dynamic mechanical testing. The numerical study has established a very high correlation between E_{HMI} and E , and has shown that E_{HMI} could be related to E through $E_{\text{HMI}} = 0.915 * E - 60$ (Pa). E_{HMI} underestimates therefore E , which is partially related to the assumption that compressive and axial strains are equal ($\epsilon_{zz} = \epsilon_{rz}$). As illustrated in table 1, these two strains were found to be slightly different. Using both ϵ_{zz} and ϵ_{rz} in equation (5) allows to decrease the difference between E and E_{HMI} . However, measuring ϵ_{rz} would be particularly challenging as it would require ultrasound imaging with very high lateral resolution in order to properly estimate lateral derivatives of the displacement. Therefore, our method here proposed to measure only ϵ_{zz} , which can be achieved by using only a single-element ultrasound imaging transducer.

The robustness of E_{HMI} was shown to be independent of the heterogeneity of the medium as long as the heterogeneity remained more than approximately 6 mm in size. This threshold value is valid for the focal size used in this study, i.e. a cylinder of 3 mm in height by 1.5 mm in diameter. Additional simulations were performed by varying the size of the focus, and preliminary results indicate that the threshold value is approximately equal to twice the height of the focal region for this cylindrical geometry (see appendix). However, the exact relationship between this threshold and the focal size needs to be further investigated. To summarize, E_{HMI} can be computed locally and independently of the elasticity distribution around the focal point, as long as the typical inclusion size is larger than approximately twice the height of the focal region. Such independence makes the method particularly robust.

Experimentally, high correlation was found between E_{HMI} and E on polyacrylamide phantoms, and they could be related linearly through $E_{\text{HMI}} = 0.83 * E + 511$ (Pa). The standard

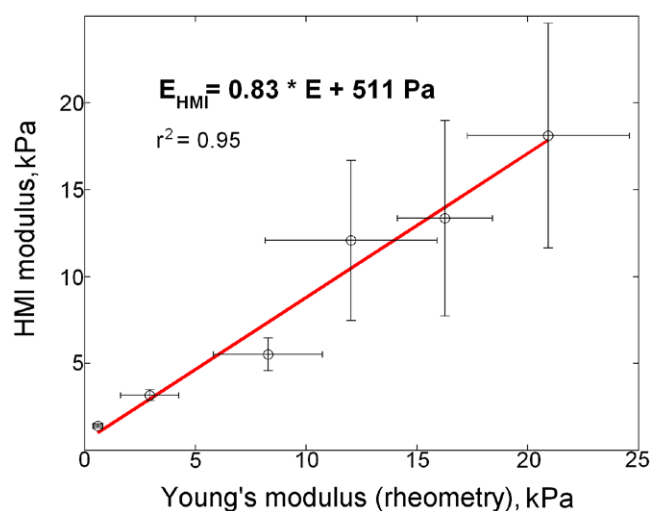


Figure 6. HMI modulus versus Young's modulus measured by rheometry on the six polyacrylamide phantoms ($N = 5-8$ for each phantom). Vertical and horizontal errorbars denote standard deviations among the different samples tested by HMI and rheometry, respectively.

Table 2. Estimated E_{HMI} on liver samples.

Specimen #	Axial strain	E_{HMI} (kPa)
1	0.011 ± 0.0025	2.98
2	0.014 ± 0.002	2.34
3	0.011 ± 0.003	2.98
4	0.016 ± 0.006	2.05
5	0.012 ± 0.005	2.73
Average	0.0125 ± 0.002	2.62 ± 0.41

Table 3. Young's modulus of *ex vivo* liver tissue measured using mechanical testing.

Specimen #	Estimated E (kPa)
1	2.64
2	2.19
3	2.16
4	7.29
5	6.72
Average	4.2 ± 2.58

deviation of the measurements was significant, especially in the most rigid phantoms (30, 35 and 40% concentration) because the estimated strain values and hence the strain signal to noise ratio were lower than that of the softer phantoms. In order to overcome this uncertainty and enhance the accuracy of the method, the input force can be increased so that the SNR also increases. However, in this phantom study, the same input force was used for all the phantoms in order to allow direct comparison in the same conditions.

Preliminary HMI modulus studies using *ex vivo* specimens were performed on liver in order to demonstrate the feasibility of the method on soft tissue. E_{HMI} and $E_{\text{MechTesting}}$ were found

to be significantly different (2.62 ± 0.41 kPa and 4.2 ± 2.58 kPa, respectively). However, experiments were performed on a very limited number of samples ($N = 10$ in total), and this conclusion should be considered with caution, especially since the inter-sample variability was found to be particularly high in mechanical testing. This can be explained by the difficulty in performing reproducible experiments on excised tissue samples: obtaining uniform, regular cylindrically-shaped samples and ensuring same conditions of tissue/plate adherence becomes particularly challenging under the same boundary conditions. The differences between our method and other conventional mechanical testing should be more thoroughly investigated on a much larger number of samples. Despite these differences that require further investigation, these preliminary *in vitro* studies demonstrate the feasibility of measuring the elasticity of biological tissues with the proposed methodology.

In this study, we demonstrated that this method was capable of providing quantitative measurements of the Young's modulus using a principle similar to indentation. This is unique in so far as our method allows to perform such indentation non-invasively, directly inside the tissue, as opposed to superficial, conventional indentation methods. Compared to quantitative shear wave elasticity imaging methods, including those based on the HMI principle (Vappou *et al* 2009), it allows to estimate elasticity directly at the focal region at a submillimetric scale; shear wave methods allow to map elasticity within the whole image, but their resolution is substantially poorer at typical imaging frequencies; they are also strongly related to the resolution of the inverse problem which may be a particularly complex issue in several tissues. The proposed method does not require an ultrasound imaging system: a focused ultrasound transducer and a single-element imaging transducer are sufficient to estimate the HMI modulus.

Several methods use the acoustic radiation force for estimating mechanical responses of biological tissues. For example, Acoustic Radiation Force Impulse Imaging (Nightingale *et al* 2002) and conventional HMI (Maleke *et al* 2006) entail measuring the tissue displacement resulting from an internal excitation. However, the displacement alone is only a qualitative indicator of tissue elasticity, because it is highly sensitive to boundary conditions and heterogeneity of the medium. Displacement can therefore be particularly useful for certain clinical diagnostic purposes, but it remains limited for biomechanical applications that aim at quantitatively measuring tissue elasticity.

Despite its potential and the promising opportunities our method offers in biomechanics, it is important to emphasize that this method relies on several assumptions and on very fine tuning of several parameters. From equation (7), we can see that the HMI modulus estimation relies first on an accurate knowledge of the applied force. The force profile can be easily obtained by a calibration process as used in this study. However, obtaining the magnitude of this force is a more complex issue. As illustrated in equation (8), the value of the force is related to the knowledge of the local tissue absorption. The uncertainty of our HMI modulus estimate will simply be proportional to any uncertainty in this value of absorption. Whereas such an acoustic parameter has been characterized on a large variety of tissues by different authors in the literature, there will always be some degree of uncertainty related to a particular given tissue. Knowing the absorption at the focal region is not the only issue: estimating correctly the pressure at the focus assumes that the energy lost in the tissue before reaching the focal region is known, which raises the question of *in situ* actual pressure versus pressure measurements obtained in a water bath. In our *ex vivo* experiments, the focal region was at a depth of 1.5 cm. We have taken into account 1.5 cm of absorption in tissue when compared to the values that were calibrated in a water bath. However, this may be more complex when applied *in vivo*, where ultrasound beams propagate through several layers of different tissues. Accurate measurement of the attenuation is necessary in order to obtain an accurate estimation of acoustic intensity at the focus. Our group has recently shown that HMI can be

used to evaluate HMI displacement attenuation, which can be used to approximate acoustic attenuation in soft tissues (Chen *et al* 2012). Once we assume that we know the applied force, other experimental parameters have to be finely tuned as well. The HMI modulus is calculated from the experimentally-measured axial strain. The estimation of this strain is related to both the quality of the displacement estimates, the axial resolution and the kernel of the Savitzky–Golay filter. With our experimental setup, we have determined that a window of ~1 mm with 90–95% overlap for the displacement estimation yielded reproducible and robust results. However, increasing this window beyond a certain degree would introduce averaging effect across the depth and therefore result in underestimation of the strain. On the other hand, decreasing this window below 1 mm may lead to displacement estimation with low SNR quality. Therefore, a tradeoff (or optimized window) has to be established based on the respective beam profile of the focused ultrasound transducer and on ultrasound acquisition parameters. Furthermore, assuming a uniform cylindrical piston can also lead to substantial limitations, because the focusing quality of the transducer must be sufficiently high for such an assumption to remain valid. In other words, any environmental conditions that may affect the quality of focusing, such as secondary lobes, must be minimized as much as possible.

Finally, it is important to re-emphasize again on the importance of all of the aforementioned limitations: Although this method is able to provide quantitative elastic parameters of biological tissues, thorough calibration and tuning procedures are required for every acquisition system and environment conditions. The presence of other uncontrolled parameters such as tissue absorption results in intrinsic uncertainty of the modulus estimate. Nevertheless, after this thorough calibration process, the proposed method can be served as a new internal indentation-based approach for measuring tissue elasticity quantitatively. In addition to its value as a biomechanical testing tool, it might also be used as a HIFU therapy monitoring tool through information on tissue stiffness during the HIFU treatment.

5. Conclusion

In this work, a noninvasive, noncontact, model-independent method for the measurement of tissues elasticity is presented based on the principle of indentation by applying the principle of HMI. The method is capable of estimating the Young's Modulus from estimated focal strain values and knowledge of the applied focal force density. The method has been validated theoretically with Finite Element Analysis (FEA), and feasibility studies have been completed experimentally using both phantoms and liver specimens. Very good agreement and correlation were found between the Young's modulus and our HMI modulus in the numerical studies, and feasibility was demonstrated *ex vivo* on liver samples. Ongoing work is being carried out in investigating the relevance of E_{HMI} as a monitoring parameter for HIFU, and investigating feasibilities on *in vivo* tumor model mice as well as *ex vivo* human pathological specimen.

Conflict of interest statement

The authors declare no conflict of interests.

Acknowledgments

This study was funded by National Institutes of Health (R01-EB014496, R21-EB008521). The authors would like to thank Nora Khanarian and Dr V C Mow from the Department of Biomedical Engineering at Columbia University for assistance in mechanical tests.

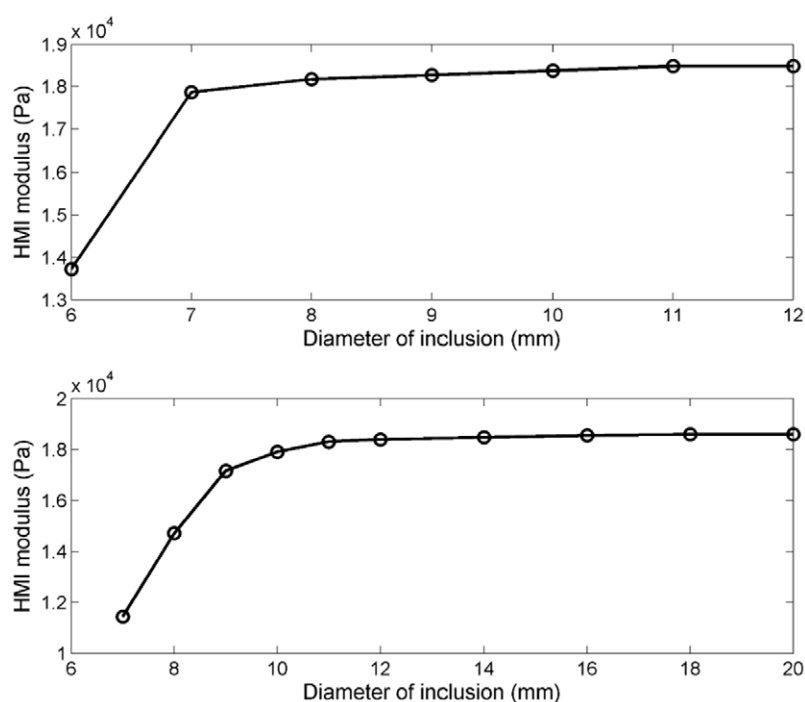


Figure A1. Effect of inclusion size on HMI modulus for scaling factor of 1.5 (top row) and 2 (bottom row).

Appendix. Effect of the size of the heterogeneity on E_{HMI} for different focus sizes

Figure 5(b) illustrates the effect of the size of the heterogeneity on the estimated HMI modulus. It is found that for inclusions larger than 6 mm in diameter, E_{HMI} is very close to the equivalent E_{HMI} found in a uniform medium (relative error <5%). For this original case, the focal size was a cylinder of 3 mm in height by 1.5 mm in diameter. The objective of this additional, preliminary study, is to assess how this threshold (equal to 6 mm in the original case) depends on the size of the focus. Similar simulations as those described in P12 and P13 (Influence of heterogeneity) were performed. Two additional configurations were tested with scaling factors of 1.5 and 2, which correspond to focal sizes of 4.5 * 2.25 mm and 6 * 3 mm, respectively.

The threshold values (relative error <5%) were found to 7 and 11 mm for the 1.5 and 2 scaling factor, respectively (figure A1). This preliminary study confirms that this threshold is in the order of magnitude of twice the length of the focal size. Ongoing work includes a more thorough investigation on the actual resolution of the proposed method, by considering different shapes and sizes of focal regions.

References

- Atay S M, Kroenke C D, Sabet A and Bayly P V 2008 Measurement of the dynamic shear modulus of mouse brain tissue *in vivo* by magnetic resonance elastography *J. Biomech. Eng.* **130** 021013
 Chen S, Fatemi M and Greenleaf J F 2004 Quantifying elasticity and viscosity from measurement of shear wave speed dispersion *J. Acoust. Soc. Am.* **115** 2781

- Chen J, Hou Y, Marquet F and Konofagou E E 2012 Radiation-force-based estimation of acoustic attenuation using harmonic motion imaging *164th Meeting of the Acoustical Society of America (Kansas City, MO)*
- Chen S, Urban M W, Pislaru C, Kinnick R, Zheng Y, Yao A and Greenleaf J F 2009 Shearwave dispersion ultrasound vibrometry (SDUV) for measuring tissue elasticity and viscosity *IEEE Trans. Ultrason. Ferroelectr. Freq. Control* **56** 55–62
- Deffieux T, Montaldo G, Tanter M and Fink M 2009 Shear wave spectroscopy for *in vivo* quantification of human soft tissues visco-elasticity *IEEE Trans. Med. Imaging* **28** 313–22
- Domire Z J, McCullough M B, Chen Q and An K-N 2009 Feasibility of using magnetic resonance elastography to study the effect of aging on shear modulus of skeletal muscle *J. Appl. Biomech.* **25** 93–7
- Fung Y C 1967 Elasticity of soft tissues in simple elongation *Am. J. Physiol.* **213** 1532–44
- Gennisson J L, Cornu C, Catheline S, Fink M and Portero P 2005 Human muscle hardness assessment during incremental isometric contraction using transient elastography *J. Biomech.* **38** 1543–50
- Green M A, Bilston L E and Sinkus R 2008 *In vivo* brain viscoelastic properties measured by magnetic resonance elastography *NMR Biomed.* **21** 755–64
- Haslach H W Jr 2005 Nonlinear viscoelastic, thermodynamically consistent, models for biological soft tissue *Biomech. Model. Mechanobiol.* **3** 172–89
- Holzappel G A, Gasser T C and Ogden R W 2000 A new constitutive framework for arterial wall mechanics and a comparative study of material models *J. Elast.* **61** 1–48
- Hou G Y, Luo J, Marquet F, Maleke C, Vappou J and Konofagou E E 2011 Performance assessment of HIFU lesion detection by harmonic motion imaging for focused ultrasound (HMIFU): a 3D finite-element-based framework with experimental validation *Ultrasound Med. Biol.* **37** 2013–27
- Jenkyn T R, Ehman R L and An K-N 2003 Noninvasive muscle tension measurement using the novel technique of magnetic resonance elastography (MRE) *J. Biomech.* **36** 1917–21
- Klatt D, Hamhaber U, Asbach P, Braun J and Sack I 2007 Noninvasive assessment of the rheological behavior of human organs using multifrequency MR elastography: a study of brain and liver viscoelasticity *Phys. Med. Biol.* **52** 7281–94
- Maleke C and Konofagou E E 2008 Harmonic motion imaging for focused ultrasound (HMIFU): a fully integrated technique for sonication and monitoring of thermal ablation in tissues *Phys. Med. Biol.* **53** 1773–93
- Maleke C, Luo J, Gamarnik V, Lu X L and Konofagou E E 2010 Simulation study of amplitude-modulated (AM) harmonic motion imaging (HMI) for stiffness contrast quantification with experimental validation *Ultrason. Imaging* **32** 154–76
- Maleke C, Pernot M and Konofagou E E 2006 Single-element focused ultrasound transducer method for harmonic motion imaging *Ultrason. Imaging* **28** 144–58
- Mariappan Y K, Glaser K J and Ehman R L 2010 Magnetic resonance elastography: a review *Clin. Anat.* **23** 497–511
- Nightingale K, Bentley R and Trahey G 2002 Observations of tissue response to acoustic radiation force: opportunities for imaging *Ultrason. Imaging* **24** 129–38
- Oliver W C and Pharr G M 1992 Improved technique for determining hardness and elastic modulus using load and displacement sensing indentation experiments *J. Mater. Res.* **7** 1564–80
- Palmeri M L, Wang M H, Dahl J J, Frinkley K D and Nightingale K R 2008 Quantifying hepatic shear modulus *in vivo* using acoustic radiation force *Ultrasound Med. Biol.* **34** 546–58
- Pattison A J, Lollis S S, Perriñez P R, Perreard I M, McGarry M D J, Weaver J B and Paulsen K D 2010 Time-harmonic magnetic resonance elastography of the normal feline brain *J. Biomech.* **43** 2747–52
- Sakuma I, Nishimura Y, Chui C K, Kobayashi E, Inada H, Chen X and Hisada T 2003 *In vitro* measurement of mechanical properties of liver tissue under compression and elongation using a new test piece holding method with surgical glue *Lect. Notes. Comput. Sci.* **2673** 284–92
- Sarvazyan A P, Rudenko O V, Swanson S D, Fowlkes J B and Emelianov S Y 1998 Shear wave elasticity imaging: a new ultrasonic technology of medical diagnostics *Ultrasound Med. Biol.* **24** 1419–35
- Schmitt C, Hadj Henni A and Cloutier G 2011 Characterization of blood clot viscoelasticity by dynamic ultrasound elastography and modeling of the rheological behavior *J. Biomech.* **44** 622–9
- Sneddon I N 1965 The relation between load and penetration in the axisymmetric boussinesq problem for a punch of arbitrary profile *Int. J. Eng. Sci.* **3** 47–57
- Vappou J 2012 Magnetic resonance—and ultrasound imaging—based elasticity imaging methods: a review *Crit. Rev. Biomed. Eng.* **40** 121–34

- Vappou J, Breton E, Choquet P, Willinger R and Constantinesco A 2008 Assessment of *in vivo* and post-mortem mechanical behavior of brain tissue using magnetic resonance elastography *J. Biomech.* **41** 2954–9
- Vappou J, Maleke C and Konofagou E E 2009 Quantitative viscoelastic parameters measured by harmonic motion imaging *Phys. Med. Biol.* **54** 3579–94
- Viola F, Kramer M D, Lawrence M B, Oberhauser J P and Walker W F 2004 Sonorheometry: a noncontact method for the dynamic assessment of thrombosis *Ann. Biomed. Eng.* **32** 696–705
- Zhai L, Palmeri M L, Bouchard R R, Nightingale R W and Nightingale K R 2008 An integrated indenter-ARFI imaging system for tissue stiffness quantification *Ultrason. Imaging* **30** 95–111